



Mechanical properties and stress distribution in aluminium 6063 extrudates processed by equal channel angular extrusion technique

Temitayo Mufutau Azeez, Lateef Owolabi Mudashiru, Tesleem Babatunde Asafa, Adekunle Akanni Adeleke, Adeyinka Sikiru Yusuff & Peter Pelumi Ikubanni

To cite this article: Temitayo Mufutau Azeez, Lateef Owolabi Mudashiru, Tesleem Babatunde Asafa, Adekunle Akanni Adeleke, Adeyinka Sikiru Yusuff & Peter Pelumi Ikubanni (2023) Mechanical properties and stress distribution in aluminium 6063 extrudates processed by equal channel angular extrusion technique, Australian Journal of Mechanical Engineering, 21:4, 1326-1334, DOI: [10.1080/14484846.2021.2003003](https://doi.org/10.1080/14484846.2021.2003003)

To link to this article: <https://doi.org/10.1080/14484846.2021.2003003>



Published online: 16 Nov 2021.



Submit your article to this journal [↗](#)



Article views: 217



View related articles [↗](#)



View Crossmark data [↗](#)



Citing articles: 2 View citing articles [↗](#)

Mechanical properties and stress distribution in aluminium 6063 extrudates processed by equal channel angular extrusion technique

Temitayo Mufutau Azeez^{a,b}, Lateef Owolabi Mudashiru^b, Tesleem Babatunde Asafa^b, Adekunle Akanni Adeleke^c, Adeyinka Sikiru Yusuff^d and Peter Pelumi Ikubanni^c

^aDepartment of Mechanical and Mechatronics, Afe Babalola University, AdoEkiti, Nigeria; ^bDepartment of Mechanical Engineering, Ladok Akintola University of Technology, Ogbomoso, Nigeria; ^cDepartment of Mechanical Engineering, Landmark University, Omu-Aran, Nigeria; ^dDepartment of Chemical and Petroleum Engineering, Afe Babalola University, Ado Ekiti, Nigeria

ABSTRACT

This study investigated the effect of temperature and load on the mechanical properties and stress distribution in ECAE processed Al6063. Samples were extruded at temperatures of 350, 425 and 500 under applied loads of 1000, 1100 and 1200 kN and ram speed of 5 mm/s. Hardness and tensile strength of all the extrudates were measured with Rockwell hardness tester and universal testing machine, respectively. Stress distribution in the extrudates was simulated with qform software under different extended applied loads and temperatures. Experimental results showed that billet temperature influenced tensile strength and hardness more significantly than applied load. The grains in the extrudates also became more refined as billet temperature increased. Simulation results indicated that more uniform stress distribution with lower magnitude was observed in the extrudates with increased billet temperature. The hardness and tensile strength of the extrudates as revealed through the uniform stress distribution were enhanced.

ARTICLE HISTORY

Received 24 October 2020
Accepted 2 November 2021

KEYWORDS

Tensile strength; hardness; extrusion; simulation; temperature

1. Introduction

Aluminium is the second most common raw material for engineering applications because of its unique properties such as good thermal and electrical conductivity, light weight, and corrosion resistance, among others (Esezobor and Adeosun 2006). These properties are responsible for their wide applications in construction, aviation, home equipment, manufacturing and marine industries. However, components made from aluminium usually have poor fatigue strength and low heat resistance, partially due to non-uniform stress distribution within the components (Nurul and Syahrullahi 2014). Many attempts have been made to improve the mechanical and metallurgical properties of aluminium-based products. One of these approaches is extrusion, which involves forcing out metal through a die with the aid of a punch under an applied load usually supplied by a hydraulic press (Weertzman 1993). Extrusion requires plastic deformation and subsequent transformation of aluminium into various shapes based on the die design (Mohan, Santhosh, and Venkata 2013). During this process, extruded products are impacted by significant changes in mechanical and metallurgical properties (Rusz and Malanik 2007).

Of all the extrusion processes, Equal Channel Angular Extrusion (ECAE) seems to be the most preferable (Seung et al. 2002). ECAE enables fine

grain structures to be obtainable in a single pass because of severe plastic deformation (Murty and Ramulu 2009). In the ECAE configuration, the die's dual channels have the same cross-sectional area and intersect at an angle of 90° to 150°. When a specimen (also known as a billet) is pressed using the angled channel of the die under high pressure, deformation occurs (Raghavan et al. 2006). The product that comes from the die after the extrusion process has an identical cross-sectional area as the initial sample (Parshikov et al. 2013), which allows multiple numbers of extrusions with a singular die and can be very advantageous in several industrial applications that demand a finer grain texture and structure in the bulk material (Roschowski 2005).

Several articles reported that the ultra-fine grain materials produced by ECAE can simultaneously combine high ductility and strength at the same time. Grain refining by severe plastic deformation can result in a unique mix of strength and ductility in metals, according to Mohammed and Senthil (Mohammed and Senthil 2016). Outstanding mechanical properties of this kind are highly appealing in the creation of next-generation innovative structural materials. However, achieving these properties necessitates post processing in order to produce a unique microstructure that improves the material's ductility (Xu 2006).

Uneven shear strain distribution, excessive extrusion load demands, and expensive procedures are all characteristics of ECAE products (Ahmed 2008). These issues arise due to non-uniform stress distribution in extrudates, resulting in decreased capacity utilisation and, as a result, higher total costs. These issues could be as a result of the disparity between billet temperature and extrusion load. The material under study may be destroyed if either the extrusion load or the billet temperature is unnecessarily high, resulting in increased process time and production expenses (Avitzur 2007). In addition, inadequate temperature or load lowers product quality, such as hardness (Seung et al. 2002). This work therefore investigated the stress distribution of Al 6063 extruded under different loads and at different temperatures by deploying both experimental and modelling approaches.

2. Materials and methods

Aluminium 6063 samples were obtained from First Aluminium Company in Lagos, Nigeria, and were cut into billets ($11.95 \times 11.95 \times 40 \text{ mm}^3$) (Figure 1 (a)). The billets were milled to obtain smooth surface finish (Figure 1(b)). The chemical compositions of the parent material were analysed using Glow Discharge Mass Spectrometer (PEM 2380). The size of the billet was chosen to allow sufficient clearance against the ECAE die of $12 \times 12 \times 58 \text{ mm}^3$ (square cross section)

with a channel angle of 120° (Figure 2(a)). The specimens were cleaned, fed into the electric furnace and heated to the selected temperatures of 350°C , 425°C and 500°C . These temperatures were selected to fall between the recrystallisation and melting temperatures of Al 6063 which are 300°C and 660°C , respectively. At these temperatures, recrystallisation occurs without melting. The heated billets were then inserted into the already lubricated ECAE die. The punch (Figure 2(b)) was coupled with the ECAE die to force the billet out of the die. The complete assembly of the billet, punch and die (Figure 2(c)) was placed in the hydraulic press (BTM 500) under varying loads (1000, 1100 and 1200 kN). Table 1 shows the range of extrusion factors and the number of extrusion passes considered for the experimental study. The selection of these factors for each experiment was based on the 20 experimental runs (Table 2) obtained from the Response Surface Methodology (RSM) which is a component of Design-Expert software.

2.1. Tensile strength and hardness test

Both the tensile strength and hardness of the aluminium 6063 extrudates were measured thrice and the mean of the values were computed for further analysis. For the tensile test, samples were machined following the ASTM B221M standard and tested on the Universal Testing Machine (Model-Accurate -10).

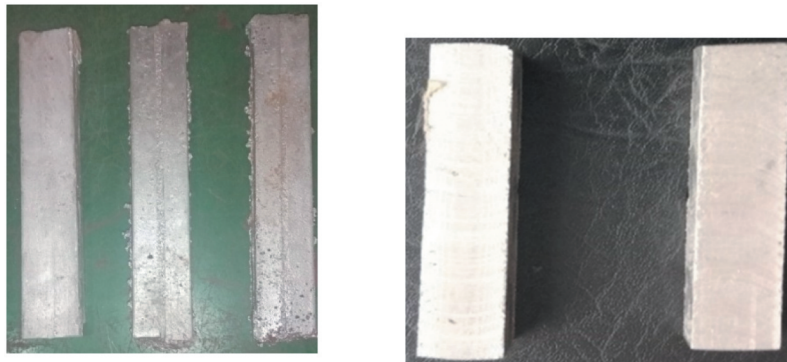


Figure 1. Aluminum samples(a) before machining, (b) after machining.

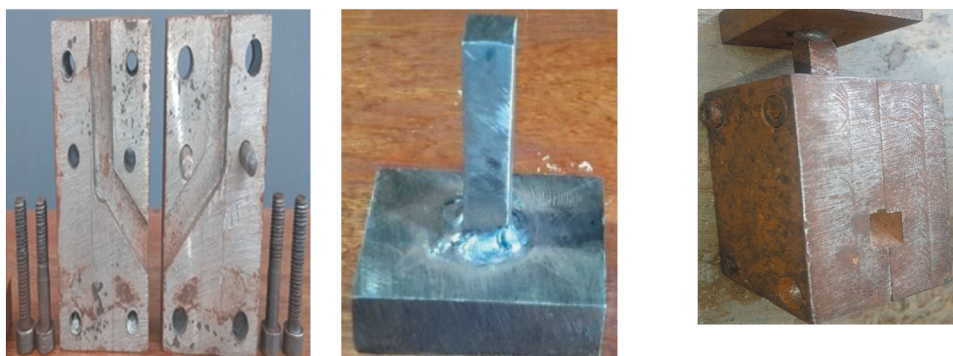


Figure 2. ECAE components (a) die (b) Punch. The assembly for the die is shown in (c).

Table 1. Extrusion factors and levels.

Factors	Code	Level		
		-1	0	+1
Passes number	N	1	2	3
Temperature of billet (°C)	T	350	425	500
Extrusion Load (kN)	L	1000	1100	1200

Table 2. Experiment layout.

S/N	Coded Value			Original Value		
	L	T	N	L (kN)	T (°C)	N
1	-1	-1	-1	1000	350	1
2	+1	-1	-1	1200	350	1
3	-1	+1	-1	1000	500	1
4	+1	+1	-1	1200	500	1
5	-1	-1	+1	1000	350	3
6	+1	-1	+1	1200	350	3
7	-1	+1	+1	1000	500	3
8	+1	+1	+1	1200	500	3
9	-1	0	0	1000	425	2
10	+1	0	0	1200	425	2
11	0	-1	0	1100	350	2
12	0	+1	0	1100	500	2
13	0	0	-1	1100	425	1
14	0	0	+1	1100	425	3
15	0	0	0	1100	425	2
16	0	0	0	1100	425	2
17	0	0	0	1100	425	2
18	0	0	0	1100	425	2
19	0	0	0	1100	425	2
20	0	0	0	1100	425	2

The Rockwell hardness testing machine (Model-Accurate FH8 900–391 C) was used for the investigation of samples' hardness. A smooth surface finish was achieved by grinding and polishing the samples before being mounted on a Rockwell hardness testing machine where the hardness values were obtained.

2.2. Response surface methodology input-output parameters modelling

The response surface quadratic model was used in connecting the input factors (numbers of extrusion passes, extrusion load and billet temperature) to the responses (hardness and tensile strength). As stated in Equation (1), the model takes into account all linear to linear connections, linear terms and square terms (Kolakoti et al. 2020).

$$Y = \beta_0 + \varepsilon \sum_{i=1}^k \beta_i x_i + \sum_{i=1}^k \beta_{ij} x_i x_j + \sum_{i=1}^k \beta_{ii} x_i^2 + \varepsilon \quad (1)$$

where Y , $\beta_i, \beta_0, \beta_{ii}, \beta_{ij}, \varepsilon$ are response, input factors linear effect, total average, input factors quadratic effect, linear to linear relation and random error respectively.

Multiple regression mathematical model of second order best fittings was generated and these were used for the analysis of the responses. Individual response analysis of variance (ANOVA) was used for the evaluation of model significance terms. Investigation of

model adequacies was carried out by evaluating prediction error sum of square (PRESS), correlation factor (R^2), predicted R^2 and adjusted R^2 .

2.3. Simulation of the ECAE process

ECAE process simulation was carried out on the *qform* platform – a professional finite element-based software dedicated to simulation, analysis, and optimisation of metal forming processes. During the simulation, the stress distribution within the extrudates and the extrusion load at various temperatures and loads were analysed. The simulation process consists of three stages: preprocessing, processing, and post-processing. At the preprocessing stage, configurations similar to those used in the experiments were produced, while few conditions were imposed, such as an assumption of homogeneous and isotropic with visco-plastic deformation. The hydraulic press provided compressive force at an extrusion rate of 0.05 m/s while friction between the work-piece and the die was considered negligible due to the added lubricant. A plane strain condition was applied and the cooling medium was air.

According to Nickolay et al. (Nickolay, Sergey, and Alexey 2014), the general material flow formulation for extrusion in the *qform* platform consists of the dynamic equation (Equation (2)), the compatibility condition (Equation (3)), constitutive equation (Equation (4)), incompressible equation (Equation (5)), energy balance equation (Equation (6)) and flow stress (Equation (7)) as presented.

$$\sigma_{ij,j} = 0 \quad (2)$$

$$\varepsilon_{ij} = \frac{1}{2} (V_{i,j} + V_{j,i}) \quad (3)$$

$$\sigma_{ij} = \frac{2\bar{\sigma}}{3\bar{\varepsilon}} \varepsilon_{i,j} \quad (4)$$

$$V_{i,i} = 0 \quad (5)$$

$$\rho c T = (T_i)_{,i} + \beta \bar{\sigma} \bar{\varepsilon} \quad (6)$$

$$\bar{\sigma} = \bar{\sigma}(\bar{\varepsilon}, \dot{\bar{\varepsilon}} T) \quad (7)$$

Where: $\sigma_{ij}, \varepsilon_{ij}, V_{i,j}$ are stress, strain rate and velocity components respectively

$\bar{\sigma}, \bar{\varepsilon}, \dot{\bar{\varepsilon}}$ are effective stress, effective strain and effective strain rate respectively

ρ, c, k are density, specific heat and thermal conductivity respectively

T is the temperature, and β is the heat generation efficiency usually assumed as 0.9–0.95

The input parameters considered for the simulation are load and temperature that was obtained from ECAE experiment conducted earlier. The die angle considered in the simulation was 120°(Roschowski 2005) while the billet (aluminium) was loaded with 1000, 1100 and 1200 kN at 350, 425 and 500°C, respectively (Table 1).

3. Result and discussion

3.1. Tensile strength and hardness

Table 3 shows the elemental composition of the aluminium 6063 sample. The result conforms with the standard aluminium 6063 sample having 0.6% Mg as the major alloying element. The hardness and tensile strength of the samples extruded at various temperatures and applied loads are presented in Table 4. The tensile strength varies between 246 and 303 MPa compared to 243 MPa for the parent material. At a billet temperature of 350°C, the tensile strengths are 250, 246 and 251 MP for applied loads of 1000, 1100 and 1200kN, respectively, given an insignificant maximum difference of 5MPa. Ditto for other temperatures. However, when the load was kept constant at 1000 kN, the tensile strengths were 250, 298 and 303 MPa for extrusion conducted at 350°C, 425°C and 500°C, respectively, indicating a maximum difference of 53MPa. Similarly, tensile strengths of 246, 286, and 302 MPa are obtained for a load of 110 kN and 251, 295, and 303 MPa

Table 3. Result of chemical composition of aluminium 6063.

Alloying Element Composition (wt %)	Si	Fe	Cu	Mn	Mg	Cr	Zn	Ti	Sr
	0.45	0.35	0.03	0.4	0.6	0.07	0.04	0.06	0.05

Table 4. Tensile and hardness as a response to load and temperature.

S/N	Original Value			Responses	
	Load (kN)	Temp (°C)	No of Passes	TS (MPa)	Hardness (HRB)
	Sample before extrusion			243	82
1	1000	350	1	250	92
2	1200	350	1	251	93
3	1000	500	1	303	110
4	1200	500	1	303	110
5	1000	350	3	258	98
6	1200	350	3	259	99
7	1000	500	3	312	113
8	1200	500	3	310	114
9	1000	425	2	298	102
10	1200	425	2	295	100
11	1100	350	2	246	94
12	1100	500	2	302	108
13	1100	425	1	286	96
14	1100	425	3	302	104
15	1100	425	2	293	102
16	1100	425	2	296	100
17	1100	425	2	296	97
18	1100	425	2	297	102
19	1100	425	2	297	101
20	1100	425	2	292	101

for a 1200 kN load at the three levels of temperature. This implies that the extrusion temperature influences the mechanical properties of extrudates more significantly than the applied load because of the wide margin observed in the value of tensile strength when temperature was varied compared to when load was varied. The significance of extrusion temperature over applied load on the hardness and tensile strength is obvious.

Similarly, the hardness values fall in the range of 92–110 HRB compared to 82 HRB for the parent material. Hardness has the same trend as tensile strength. The hardness values at a constant temperature of 350°C for 1000, 1100, and 1200 kN load are 92, 94, and 93HRB, respectively, indicating less influence of extrusion load. At 1000 kN, the hardness values are 92, 102, and 110 HRB at extrusion temperatures of 350, 425, and 500°C, respectively, confirming the significant influence of temperature (Arty, Ze'ev, and Frage 2020). The greater influence of extrusion temperature over load may be as a result of recrystallisation and grain growth at higher temperatures (Namrata, Sanchin, and Arshad 2017). At this temperature, grain structures are refined into ultrafine grains with many grain boundaries that naturally resist movement of dislocation during deformation, and hence the enhanced properties observed (Nemati et al. 2015).

3.2. Empirical model

The behavioural description of response to the input factors was carried out by using second-order polynomial of the type stated in Equation (1). Equation (1) can further be transformed into Equation (8) when considering the three variables used in this study.

$$Y = X_0 + X_1(A) + X_2(B) + X_3(C) + X_{11}(A^2) + X_{22}(B^2) + X_{33}(C^2) + X_{12}(AB) + X_{13}(AC) + X_{23}(BC) \tag{8}$$

Where all X are constants and Y is the response

The generated model equations based on the coded factors are given as Equations (9) and (10) for tensile strength and hardness, respectively.

$$Y_1(\text{MPa}) = \{295.56 - 0.34A + 24.75B + 4.63C - 0.50AB - 0.25AC + 0.000BC + 5.246E - 003A^2 - 12.98B^2 - 1.43C^2\} \tag{9}$$

$$Y_2(\text{HRB}) = \{100.2 + 0.32A + 7.28B + 2.57C - 0.12AB + 0.13AC - 0.063BC + 1.23A^2 + 1.23B^2 + 0.65C^2\} \tag{10}$$

Y₁, Y₂, A, B and C are Tensile strength response, hardness response, load, temperature and number of passes respectively.

Table 5. Determination of model significance using ANOVA.

Source	Tensile Strength		Hardness	
	F Value	p- value	F Value	p-value
Model	91.73	< 0.0001	15.37	< 0.0001
A-load	0.13	0.7252	0.00	0.9630
B-temperature	674.75	< 0.0001	116.49	< 0.0001
C-no of pass	23.61	0.0007	14.60	0.0034
AB	0.19	0.6704	0.02	0.8800
AC	0.05	0.8309	0.02	0.8800
BC	0.00	1.0000	0.60	0.4566
A ²	0.00	0.9967	2.03	0.1846
B ²	112.98	< 0.0001	2.03	0.1846
C ²	1.37	0.2684	0.56	0.4700

3.3. Model significance

In the reliability [Table 5](#), factors significance are determined by analysis of model adequacy using ANOVA (when $p \leq 0.05$ and insignificant if otherwise) (Aydin, Uslu, and Celik 2020). As a result, the generated models are significant. Considering p-value for all the input factors, temperature (B) is the most significance factor while load (A) is the least.

Table 6. Second order model fitting result in form of ANOVA.

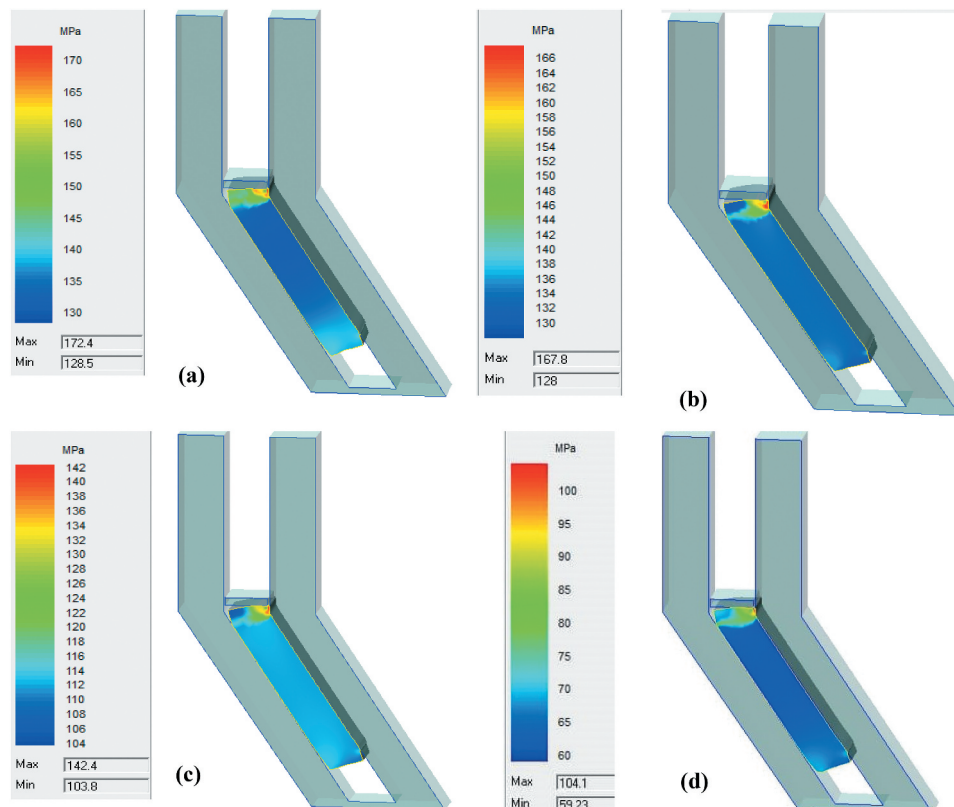
Model Summary characteristics	Tensile Strength	Hardness
Standard Deviation	3.23	3.37
R ²	0.9880	0.9836
Adjusted R ²	0.9773	0.9617
Predicted R ²	0.9257	0.9079
PRESS	645.61	648.55
Adeq Precision	31.72	12.28
F-Value	P = 0.0949	P = 0.2361

3.4. Model fitting analysis

The conditions for an excellent fit are that the coefficient of determination (R^2) must be greater than or equal to 95%, the variation between predicted R^2 and adjusted R^2 must be less than or equal to 10%, adequate precision must be greater than 4 and insignificant lack of fit (F-Value) (Azeez et al. 2021). As indicated in [Table 6](#), R^2 of 0.9880 and 0.9836 for both tensile strength and hardness and the variation between adjusted R^2 and predicted R^2 of 5.16% and 5.38 indicate a good fit. Other variables also support the fact that the model is adequate and reliable, and can be used to navigate design space

3.5. Simulation result and temperature effects on the stress developed

In all the models, the effect of thermal stress was neglected because the samples were heated in a furnace where free expansion was allowed. If the billets were heated in a constrained environment, as much as 764 MPa (at 500°C) of thermal stress would have been induced (Wojciech and Tomasz 2013). This indicates that the observed stress distribution in the post-extrusion billet is due to the applied load. [Figure 3\(a-c\)](#) shows the stress distribution in the billets after extrusion at designated temperatures of 350, 425 and 500°C and a constant load of 1000 kN. The maximum stress decreased with increased extrusion temperature, implying that temperature lowers the stress level.

**Figure 3.** Flow stress distribution in samples extruded at temperature of (a) 350°C (b) 425°C (c) 500°C and (d) 550°C.

According to Winholtz (Winholtz 2001), metal yield strength decreases because of increased thermal stress occasioned by high temperatures. At such a temperature, the metal undergoes microscopic plastic deformation, thereby releasing a portion of the residual stresses.

The increased flow stress at 350°C compared to the stress prior to extrusion is due to the plastic deformation of the billet (Keste and Sarkar 2016). Except at the top edges of the extrudates, where a maximum stress of 172 MPa was observed, the flow stress is largely uniform between 130 and 135 MPa (Figure 3(a)). At a higher extrusion temperature of 425°C, the maximum and minimum stress levels were reduced to 167.8 and 128 MPa, respectively (Figure 3(b)). Ditto for extrusion at 500°C, in which the maximum and minimum stress levels were 142.4 and 103 MPa, respectively (Figure 3(c)). At 550°C, the stress level reduced drastically to 59 and 104 MPa for the minimum and maximum levels, respectively (Figure 3(d)). The observed reduction in the stress level with temperature is depicted in Figure 4(a), which shows a significant change as the extrusion temperature approaches the melting point of aluminium (660°C) (Namrata, Sanchin, and Arshad 2017). The figure also points to the high-level impact of temperature as a major factor in the ECAE process, especially for aluminium alloy (Zhenhua, Xianhua, and Qiangian 2004). It appears the stress distribution becomes more uniform with extrusion temperature, as seen in Figure 3. Effectively, the upper parts of the billets can be cut-off to have a product with minimal stress gradients. Such a small stress gradient produces high-strength aluminium with higher tensile strength, as observed in the experimental data in Table 4, where tensile strength increases with extrusion temperature (Maoyu et al. 2018).

Figure 4(b) shows the actual extrusion load against displacement for billets extruded at different temperatures. The deformation behaviour has three distinct stages (Nemati et al. 2014). At first, the extrusion load increases rapidly, indicating downward displacement

of the billet towards the corner of the die. This is immediately followed by the dwelling of the extrusion load, which corresponds to the steady state of the process when billets continuously pass through the corner of the die. This load actually gives the maximum extrusion load for that particular temperature. Finally, the extrusion load drops to zero, indicating the completion of the deformation process. As observed, the extrusion load decreases with increased extrusion temperature (Nickolay, Sergey, and Alexey 2014) with a maximum load of 500 kN needed for extrusion at a temperature lower than 500°C. At 500°C and beyond, the extrusion load falls drastically. For instance, while the extrusion load was reduced to 430 kN at 500°C, it fell below 260 kN at 550°C. This significant reduction in the extrusion load can be attributed to the fact that flow stress is reduced with increased temperature (Flitta and Sheppard 2005) and, by extension, the processing time is also reduced (Lontos et al. 2008).

3.6. Loading effects on stress distribution

From the simulation performed thus far, using an applied load higher than 500 kN has no effect on the extrusion load of the ECAE process while the stress distribution is marginally affected. This is confirmed in Figure 5(a,b) where the stress distribution for extrusion conducted at 350°C under 700 kN and 1000 kN differ by just 10 MPa with higher stress obtained at 700 kN. Also, the stress distribution seems to be more uniform at 700 kN, compared to 1000 kN probably because of the lower deformation rate and consequent lower strain gradient as observed elsewhere (Jandrlic et al. 2018). Figure 5(c-d) also confirms that the extrusion loads are the same despite the huge difference in the applied load provided the extrusion temperature remains constant. At 350°C, applied loads of 700, 1000, 1100, and 1200 kN have the same extrusion load as 500 kN. However, at 500°C, the same set of applied loads has an extrusion load of 430 kN.

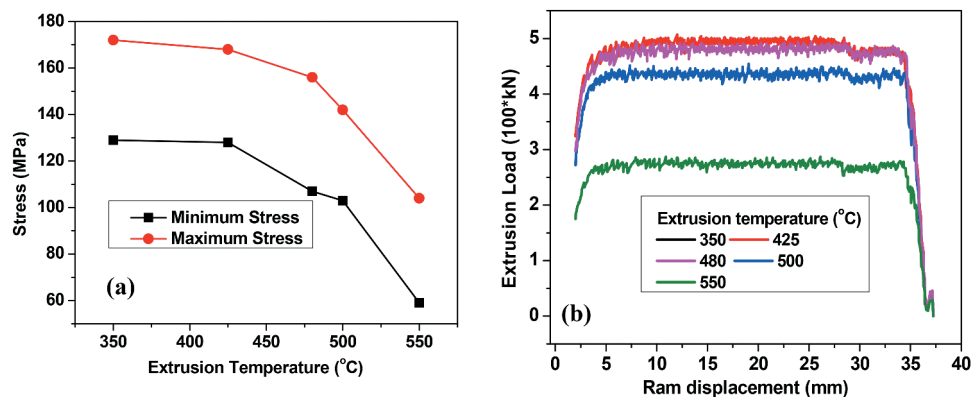


Figure 4. (a) Stress against extrusion temperature (b) extrusion load – ram displacement curves for extrusion carried out under an applied load of 1000 kN at different temperatures. Curves corresponding to 350°C and 425°C overlapped.

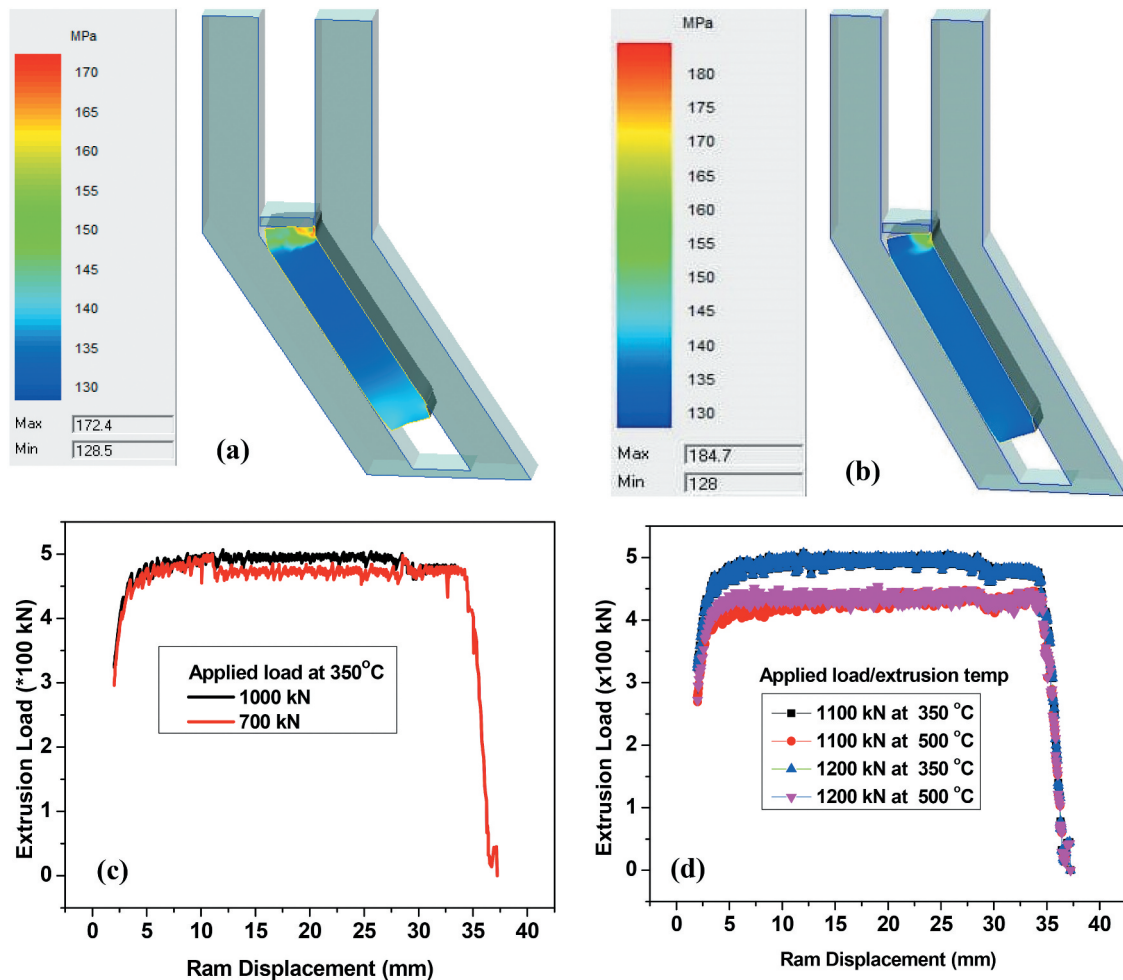


Figure 5. Stress distribution in samples extruded at 350°C under an applied load of (a) 1000 kN (b) 700 kN. The extrusion load – displacement curve is shown in (c). (d) extrusion load – ram displacement curves for extrusion carried out under an applied load of 1100/1200 kN at two temperature regimes.

Theoretically, the maximum extrusion load for the aluminium billet processed at the recrystallisation temperature of 350°C is 508 kN (Wang et al. 2013), which is also confirmed by the simulation results. While higher load may lower extrusion time, it does not affect the actual extrusion load, which largely determines the power consumed during the metal working process (Lontos et al. 2008).

3.7. Microscopic analysis of the extruded and parent samples

SEM images of the surface morphologies of the parent material and extrudates are shown in Figure 6. The surface structure of as-received aluminium 6063 shows severe surface damage sustained during manufacturing (Figure 6(a)). However, most of these damages were attenuated after the ECAE process at all extrusion temperatures. A closer look at Figure 6(b) shows larger coarse grains while the formation of a less coarse grain microstructure is visible at 425°C and 500°C (Figure 6(c,d)). The reduction in grain sizes is noticed as the temperature increased. This is due to the sub cell formation owing to

high dislocation density occasioned by high temperature, and thus refinement of grains takes place. As grain structures become smaller, grain boundaries increase. This impedes dislocation movement within the grains (Nemati et al. 2015). This is considered to be partially responsible for the increased strength and hardness obtained (Rusz and Malanik 2007).

4. Conclusions

This study confirmed temperature having a better influence as a process parameter in the ECAE process than load at all applied loads and temperatures. However, at a load of 700 kN, the stress increased to a maximum level of 184.7 MPa from 172 MPa under a 1000 kN load. High temperature has a load reduction capacity at a temperature of 480°C and above before melting temperature. It also enabled a more uniform stress distribution in aluminium processed by ECAE. SEM images indicate a grain size reduction of the components extruded at different temperatures compared to the parent material. Therefore, the research findings have provided baseline information for accurate predictions of aluminium

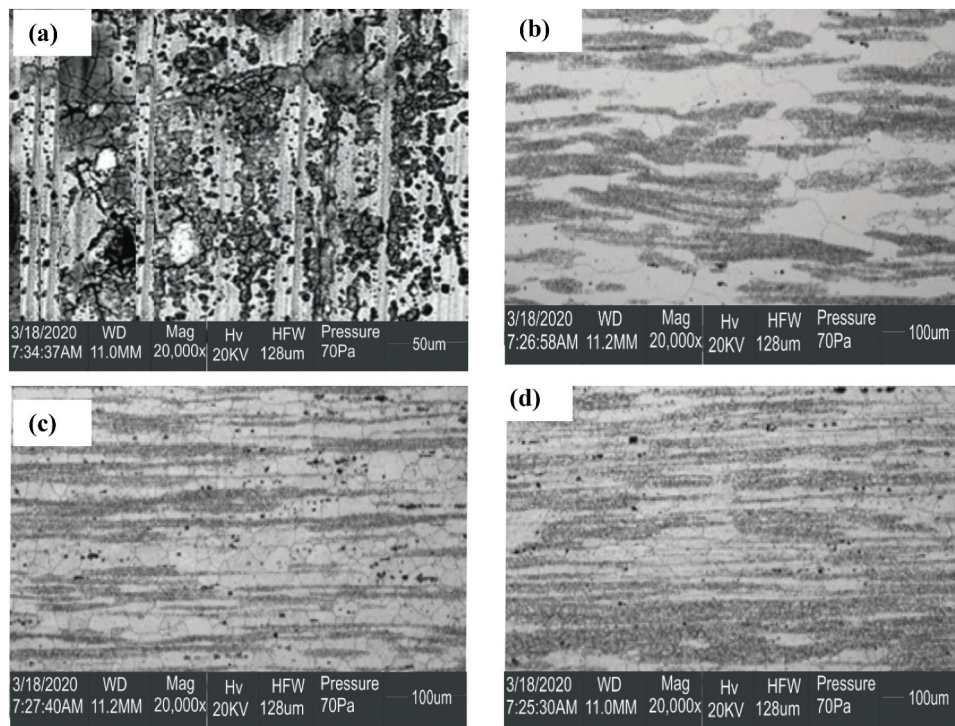


Figure 6. SEM images of (a) sample of parent material (b) sample extruded at 350°C (c) sample extruded at 425°C (d) sample extruded at 500°C.

strength and for having reliable products working within the safety limit of optimum manufacturing cost.

Acknowledgments

We appreciate the management of Afe-Babalola University, AdoEkiti, Nigeria and Ladoke Akintola University of Technology, Ogbomoso, Nigeria for making their laboratories and technologists available during this research.

Disclosure statement

All the six authors in this article hereby declare unknown any personal or financial connections that could eventually tamper with the research presented in this paper.

Notes on contributors

Dr. **T. M Azeez** is a lecturer at the Department of Mechanical and Mechatronics Engineering, Afe Babalola University Ado Ekiti, Nigeria. His research area is Industrial and material production.

Dr. **Lateef Owolabi Mudashiru** is an associate professor at the Department of Mechanical Engineering, Ladoke Akintola University of Technology, Ogbomoso, Oyo State, Nigeria. His research area is Industrial and material production.

Dr. **Tesleem Babatunde Asafa**, is an associate professor at the Department of Mechanical Engineering, Ladoke Akintola University of Technology, Ogbomoso, Oyo State Nigeria. His Area of research is material engineering and nano technology.

Adekunle Akanni Adeleke, is a lecturer at Landmark University, Omu Aran, Nigeria. His research interest is renewable energy and material characterization

Dr. **Adeyinka Sikiru Yusuff**, is a lecturer at the Department of Chemical and Petroleum Engineering, Afe Babalola University Ado Ekiti, Nigeria. His Area of research is catalysis, renewable energy and material synthesis and characterization.

Peter Pelumi Ikubanni is a lecturer at Landmark University, Omu Aran, Nigeria. His research interest is renewable energy and material characterization.

Data Availability Statement

Data available within the article

References

- Ahmed, O. 2008. "Effect of Parameters and Operating Conditions on Flow of Extrusion Load." *Scripta Materialia*, no. 14(49): 46–55.
- Arty, A. B., S. B. Ze'ev, and N. Frage. 2020. "Teaching Metal-Forming Process Using a Laboratory Micro-extrusion Press." *The Minerals, Metals and Materials Series* 55–67. doi:10.1007/978-3-030-36556-1.
- Avitzur, B. 2007. *Metal Forming Processes and Analysis*. 2nd ed. New York: Wiley Interscience.
- Aydin, M., S. Uslu, and M. B. Celik. 2020. "Performance and Emission Prediction of A Compression Ignition Engine Fueled with Biodiesel-diesel Blends: A Combine Application of ANN and RSM Based Optimization." *Fuel* 269: 1–6. doi:10.1016/j.fuel.2020.117472.

- Azeez, T. M., L. O. Mudashiru, T. B. Asafa, A. A. Adeleke, and P. P. Ikubanni. 2021. "Mechanical Properties of Al 6063 Processed with Equal Channel Angular Extrusion under Varying Process Parameters." *International Journal of Engineering Research in Africa* 54: 23–32.
- Esezobor, D. E., and S. O. Adeosun. 2006. "Improvement on the Strength of 6063 Aluminum Alloy by Means of Solution Heat Treatment." *Materials Processing Challenges Aerospace Industry*, no. (9)1: 645–655.
- Flitta, I., and T. Sheppard. 2005. "Effects of Pressure and Temperature Variations on FEM Prediction of Deformation during Extrusion." *Materials Science and Technology* 21 (3): 339–346. doi:10.1179/174328405X29221.
- Jandrljic, J., S. Reskovic, T. Brlic, and V. Furlan. 2018. "Effect of Deformation Rate on Low Carbon Steels Mechanical Properties." *Materials and Engineering*, 461 (1): 1–6.
- Keste, A. A., and C. Sarkar. 2016. "Design Optimization of Precision Casting for Residual Stress Reduction." *Journal of Computational Design and Engineering* 3 (2): 140–150.
- Kolakoti, A., P. Jha, P. R. Mosa, M. Mahapatro, and T. J. Kotaru. 2020. "Optimization and Modelling of Mahua Oil Biodiesel Using RSM and Genetic Algorithm Techniques." *Mathematical Models in Engineering* 6: 134–146. doi:10.21595/mme.2020.21357.
- Lontos, F. A., D. A. Soukatzidis, D. A. Demosthenous, and A. K. Baldoukas. 2008. "Effects of Extrusion Parameters and Die Geometry on the Produced Billet Quality Using Finite Element Method." *International Conference of Manufacturing Engineering*, Chakidiki, Greece pp. 215–228.
- Maoyu, Z., M. Zhengzheng, T. Chunyan, and L. Ping. 2018. "The Relationship between Tensile Strain and Residual Stress of High Strength Dual Phase Steel Sheet." *MATEC Web of Conferences*, France, pp. 1–5.
- Mohammed, I. U., and K. S. Senthil. 2016. "Application of Response Surface Methodology in Optimizing Process Parameters of Twist Extrusion Process for Aluminum Aa 6061- T6 Alloy." *Measurement* 94 (94): 126–138. doi:10.1016/j.measurement.2016.07.085.
- Mohan, R., M. I. Santhosh, and K. G. Venkata. 2013. "Improving Mechanical Properties of Al 7075 Alloy by Equal Channel Angular Extrusion Process." *International Journal of Modern Engineering Research* 3 (5): 2713–2716.
- Murty, D. V., and M. Ramulu. 2009. "Deformation Study of Dual Equal Channel Lateral Extrusion." *International Journal of Engineering Studies*, no. 4(3): 161–168.
- Namrata, G., M. Sanchin, and N. S. Arshad. 2017. "Multipass FSP on AA 6063- T6 Al: Strategy to Fabricate Surface Composites." *Materials and Manufacturing Processes* 15 (2): 1–7.
- Nemati, J., G. H. Majzooobi, S. Sulaiman, B. T. Baharudin, and M. A. Azmah. 2015. "Effect of Equal Channel Angular Extrusion on Al-6063 Bending Fatigue Characteristics." *International Journal of Minerals, Metallurgy, and Materials* 22 (4): 396–404. doi:10.1007/s12613-015-1085-z.
- Nemati, J., S. Sulaiman, G. H. Majzooobi, B. T. H. T. Baharudin, and M. A. Azmah. 2014. "Finite Element Study of Deformation Behavior of Al-6063 Alloy Developed by Equal Channel Angular Extrusion." *Advanced Materials Research* 1043 (1043): 119–123.
- Nickolay, B., V. Sergey, and V. Alexey. 2014. *Material Forming Simulation Environment Based on QFORM Software System*. Moscow.
- Nurul, M. A., and S. Syahrullahi. 2014. "Study of Alternative Lubricant for Cold Extrusion Process of A1100 Pure Aluminum." *Jurna Teknologgi* 71 (2): 139–143.
- Parshikov, R. A., A. I. Rudskoy, A. M. Zolotov, and O. V. Tolochko. 2013. "Technology Problem of Equal Channel Angular Pressing." *Journal Advanced Materials Science*, no. 34(24): 26–36.
- Raghavan, S., H. Qingyou, S. David, G. Percy, M. Rob, and K. Chaudhury. 2006. *Continuous Severe Plastic Deformation Processing of Aluminum Alloys Intercontinental manufacturing Co, Texas*.
- Roschowski, A. 2005. "Processing Metals by Severe Plastic Deformation." *Solid State Phenomena* 101-102 (10): 13–22.
- Rusz, R. S., and K. Malanik. 2007. "Using Severe Plastic Deformation to Prepare Ultra-fine Grained Material by ECAE Method." *Journal of Achievements in Materials Science Engineering*, no. 11(28): 683–687.
- Seung, C. B., E. H. Yuri, S. K. Hyoung, T. J. Hyo, and J. H. Raph. 2002. "Calculation of Deformation Behavior and Texture Evolution during Equal Channel Angular Pressing." *Materials Science Forum* 408: 697–702.
- Wang, X., M. Zhang, N. Tang, N. Li, L. Liu, and J. Li. 2013. "A Forming Load Prediction Model in BMG Micro Backward Extrusion Process considering Size Effect." *Physics of Non Crystalline Solid* 12(48):146–151.
- Weertzman, J. K. 1993. "Hall-petch Strengthening in Nanocrystalline Metals." *Materials Science and Engineering: A* 1 (2): 161–167. doi:10.1016/0921-5093(93)90319-A.
- Winholtz, R. A. 2001. "Residual Stresses: Macro and Micro Stresses." *Materials Science Technology*, no. 46(49):1–4.
- Wojciech, S., and L. Tomasz. 2013. "Thermal Stresses in Metallic Materials Due to Extreme Loading Conditions." *Journal of Engineering Materials and Technology* 135 (8): 1–8.
- Xu, S. 2006. "Finite Element Analysis and Optimization of Equal Channel Angular Pressing for Producing Ultra-fine Grained Materials." *Journal of Materials Processing Technology*, no. 184 (3): 209–216.
- Zhenhua, L., C. Xianhua, and S. Qiangian. 2004. "Effects of Heat Treatment and ECAE Process on Transformation Behaviour of TiNi Shape Memory Alloy." *Materials Letters*, no. 10(59): 705–709.